


Review

Breaking Left–Right Symmetry by the Interplay of Planar Cell Polarity, Calcium Signaling and Cilia

De-Li Shi 

Laboratoire de Biologie du Développement, LBD, CNRS UMR7622, INSERM U1156, Sorbonne Université, F-75005 Paris, France; de-li.shi@upmc.fr

Abstract: The formation of the embryonic left–right axis is a fundamental process in animals, which subsequently conditions both the shape and the correct positioning of internal organs. During vertebrate early development, a transient structure, known as the left–right organizer, breaks the bilateral symmetry in a manner that is critically dependent on the activity of motile and immotile cilia or asymmetric cell migration. Extensive studies have partially elucidated the molecular pathways that initiate left–right asymmetric patterning and morphogenesis. Wnt/planar cell polarity signaling plays an important role in the biased orientation and rotational motion of motile cilia. The leftward fluid flow generated in the cavity of the left–right organizer is sensed by immotile cilia through complex mechanisms to trigger left-sided calcium signaling and lateralized gene expression pattern. Disrupted asymmetric positioning or impaired structure and function of cilia leads to randomized left–right axis determination, which is closely linked to laterality defects, particularly congenital heart disease. Despite of the formidable progress made in deciphering the critical contribution of cilia to establishing the left–right asymmetry, a strong challenge remains to understand how cilia generate and sense fluid flow to differentially activate gene expression across the left–right axis. This review analyzes mechanisms underlying the asymmetric morphogenesis and function of the left–right organizer in left–right axis formation. It also aims to identify important questions that are open for future investigations.

Keywords: left–right organizer; left–right asymmetry; cilia; Wnt/PCP; calcium; polycystin; laterality defects



Citation: Shi, D.-L. Breaking Left–Right Symmetry by the Interplay of Planar Cell Polarity, Calcium Signaling and Cilia. *Cells* **2024**, *13*, 2116. <https://doi.org/10.3390/cells13242116>

Academic Editor: Lisbeth Birk Møller

Received: 18 November 2024

Revised: 7 December 2024

Accepted: 19 December 2024

Published: 20 December 2024



Copyright: © 2024 by the author. Licensee MDPI, Basel, Switzerland. This article is an open access article distributed under the terms and conditions of the Creative Commons Attribution (CC BY) license (<https://creativecommons.org/licenses/by/4.0/>).

1. Introduction

The formation of embryonic axes is a fundamental process in development. It contributes to shaping the basic body plan of bilaterian organisms. The establishment of the dorso-ventral (D–V) and antero-posterior (A–P) axes is tightly linked, which takes place before and during gastrulation. This is regulated by an interplay of conserved signaling factors that coordinate spatial–temporal gene expression patterns and morphogenetic cell movements [1,2]. The specification of the left–right (L–R) axis occurs at early stages of somite segmentation. The signaling pathways implicated in initiating the L–R pattern are also evolutionarily conserved in metazoa, but differences in the mode of their functions may exist among various species [3–6]. Although the developing vertebrate embryos seemingly show bilateral symmetry, they already possess L–R asymmetry of gene expression patterns. Importantly, the formation of the L–R axis not only breaks the mediolateral symmetry of the early embryo but also dictates the asymmetric location and morphogenesis of internal organs, which eventually display L–R differences in sizes, shapes, and anatomical dispositions. Therefore, the L–R asymmetry is a common aspect in animals [7,8], particularly in the development of visceral organs, such as the rightward looping of the heart tube and the leftward curvature of the stomach, as well as their precise positioning in the body cavity [9].

How is the L–R asymmetry initiated in the embryo? It is now well established that transient embryonic structures, including the node in mice, the Hensen’s node in chicks, the

posterior gastrocoel roof plate in *Xenopus* early neurula, and the Kupffer's vesicle (KV) in zebrafish, function as L–R organizers and produce instructive cues to break the bilateral symmetry across the mediolateral plane mostly in a cilia-dependent manner [10–13]. Thus, both motile and immotile cilia within the L–R organizers contribute to initiating the determination of the L–R asymmetry [14]. Among many molecular regulators involved in initiating the L–R asymmetry, the Wnt/planar cell polarity (PCP) pathway and calcium signaling play important conserved roles in the morphogenesis of the L–R organizer and in mediating cilia function to activate a left-sided gene expression program, respectively. Components of the Wnt/PCP pathway coordinate cellular orientations in the L–R organizer with respect to the D–V and A–P axes [9,15–18]. Subsequently, the clockwise (ventral view) rotational motion of motile cilia within the L–R organizer triggers asymmetric fluid flow and calcium flux on the left side, known as Nodal flow [10,19,20], and signals the determination of the L–R axis [21,22]. As a result, the Nodal–Lefty–Pitx2 gene network is activated on the left side [11]. This differential gene expression establishes the L–R polarity that critically contributes to positioning the asymmetric morphogenesis of organ primordia [23–25]. Because the close link between L–R axis determination and asymmetric organogenesis, disrupted formation and function of the L–R organizer can result in laterality defects such as heart malformations [26,27]. While situs solitus refers to the normal anatomy pattern, altered L–R axis development causes situs inversus, heterotaxia, or isomerism, which are congenital disorders with complete reversed, partially inverted, or symmetric positioning of visceral organs, respectively.

This review focuses on two closely linked early events essential for breaking the bilateral symmetry: Wnt/PCP signaling regulates the asymmetric positioning of motile cilia in the L–R organizer, while the leftward Nodal flow sensed by immotile cilia triggers intraciliary calcium transients to initiate L–R axis patterning. It also briefly presents the consequences of mutations affecting genes associated with the L–R organizer on congenital heart malformations. By providing an in-depth analysis of the intricate processes operating in the L–R organizer, this work offers insights into the molecular mechanisms underlying L–R axis development and asymmetric organ morphogenesis.

2. The Wnt/PCP Pathway

Wnt signaling is evolutionarily conserved and can be subdivided mainly into canonical (Wnt/ β -catenin) and non-canonical (Wnt/PCP) pathways. Wnt/ β -catenin signaling regulates gene expression and cell fate specification in a manner that is dependent on β -catenin nuclear translocation. The Wnt/PCP pathway (Figure 1A), however, controls cellular orientation within the plane of an epithelium or a tissue by regulating cytoskeletal rearrangements and/or transcriptional responses [9]. The PCP phenomenon is essentially coordinated by six “core” proteins (Frizzled, Celsr1, Vangl2, Dishevelled or Dvl, Prickle, and Ankrd6), which transduce the signal through downstream effectors including Daam1 (Dishevelled-associated activator of morphogenesis 1), small GTPases of the Rho family, and JNK (Jun N-terminal kinase). In vertebrates, several Wnt ligands (Wnt5 and Wnt11) also contribute to establishing the PCP by binding to membrane receptors (Frizzled) and co-receptors (Ror1/2 or Ryk), although they are not considered as “core” PCP proteins [28]. The “core” PCP proteins form two separate complexes that show characteristic asymmetric distribution on opposite borders of the cell within the tissue plane. Thus, Frizzled, Dvl, and Ankrd6 localize to one side of the cell, while Prickle and Vangl2 are present at the opposite side. Celsr resides on both sides of the cell and functions to propagate polarity information across cells by forming homodimers between adjacent cells (Figure 1B). This asymmetric distribution of “core” PCP protein complexes establishes planar polarization and controls cell polarity during tissue and organ morphogenesis [9,29–31].

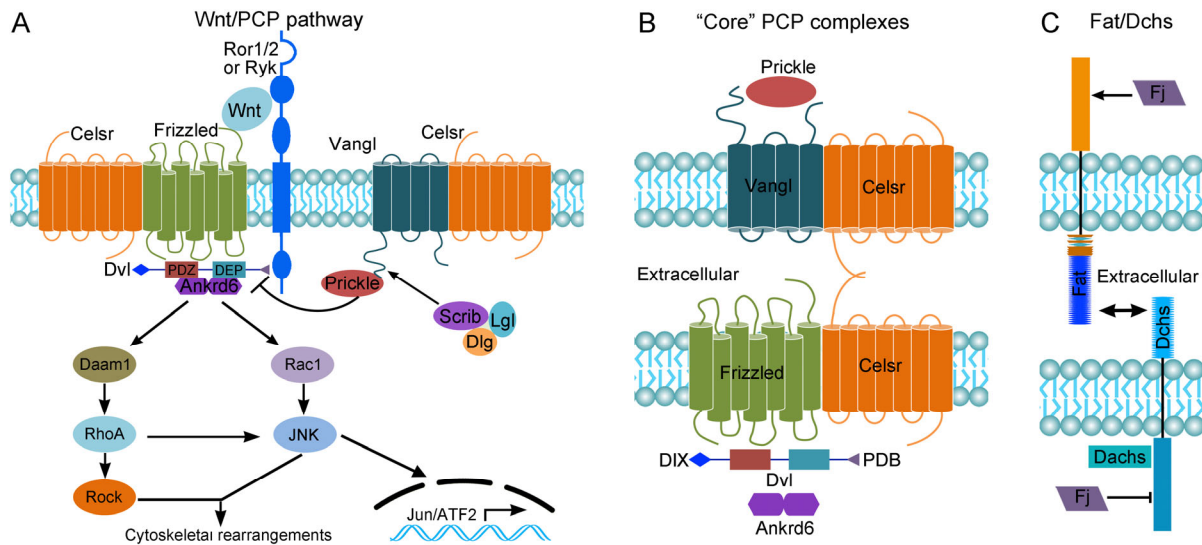


Figure 1. The Wnt/PCP pathway. **(A)** Non-canonical Wnt ligands bind to receptor and co-receptor complexes formed by Frizzled with Ror1/2 or with Ryk to activate downstream effectors via Dvl, regulating cytoskeletal rearrangements or transcriptional responses. The Scrib/Dlg/Lgl complex can regulate Vangl asymmetric localization. **(B)** Cell polarity is established by the interaction between two “core” PCP protein complexes that are distributed on opposite cell borders. Vangl and Prickle localize to the anterior side, while Frizzled, Dvl, and Ankr6 are distributed at the posterior side. Celsr is present on both sides of the cell to propagate polarity information. DIX, DIX domain; PDB, PDZ domain-binding. **(C)** The Fat/Dchs polarity module. Fat and Dchs protocadherins form heterodimers between adjacent cells and function as a ligand–receptor pair. Phosphorylation of Fat by the Four-jointed (Fj) kinase enhances its binding with Dchs, but phosphorylation of Dchs by Fj reduces its interaction with Fat. Dachs is an unconventional myosin that interacts with Dchs and functions as a key effector of Fat/Dchs signaling.

It has been proposed that there are also other conserved protein complexes acting as important PCP regulators. The heteromeric protocadherins Fat4 and dachsous cadherin-related 1 (Dchs1) are present on opposite cell borders to form a ligand–receptor pair (Figure 1C). This module is considered as the second PCP pathway, at least in *Drosophila*. It is regulated by the Golgi resident transmembrane kinase Four-jointed (Fj), which phosphorylates serine/threonine residues within the extracellular cadherin domains of Fat4 and Dchs1 as they transit through the Golgi [32]. The Scrib (Scrb1 or Scribble1) polarity complex, which consists of Scrib, Discs-large (Dlg), and Lethal-giant larvae (Lgl) proteins, was initially identified as a regulator of apico-basal cell polarity in *Drosophila*, but there is a large body of evidence suggesting that it also acts to coordinate PCP in vertebrates [33]. Therefore, these pathways function cooperatively with or independently of “core” PCP proteins to regulate cell polarity.

3. Wnt/PCP Signaling Instructs the Asymmetric Orientation of Motile Cilia in the L–R Organizer

There are two types of ciliated cells in the mouse node [13,20]. Pit cells are located within a depression at the center of the node. Their motile cilia are posteriorly tilted and rotate clockwise to produce leftward fluid flow. Crown cells are located at the periphery of the node and possess immotile cilia. Several components of the Wnt/PCP pathway are critically involved in the asymmetric morphogenesis of the vertebrate L–R organizer, and their restricted distribution makes an important contribution in breaking the bilateral symmetry [11]. In mice, Wnt5a and Wnt5b are expressed in the posterior region of the node; they produce a diffusible gradient which provides instructive signals to polarize node cells along the A–P axis by promoting the anterior localization of three “core” PCP proteins: Vangl1, Vangl2, and Prickle2 [34]. Complementary with this distribution, Dvl2 and Dvl3

are enriched at the posterior side of node cells [11,35]. As a result, this leads to a biased distribution of microtubules and actomyosin networks, thereby restricting posteriorly the positioning of ciliary basal bodies and the tilting of cilia in node cells [36]. Functional studies in different species have firmly established a critical role for PCP proteins in initiating the L–R differences. Knockout of *Dvl2* and *Dvl3* perturbs the posterior positioning of ciliary basal bodies in mouse node cells and impairs the unidirectional fluid flow [35]. Similarly, *Vangl1* and *Vangl2* are required for the posterior orientation of motile cilia in the mouse node [37–39], the zebrafish KV [40], and the *Xenopus* gastrocoel roof plate [37]. Thus, the loss of their function interferes with the left-sided expression of *Nodal*, *Lefty*, *Sonic hedgehog* (*Shh*), and *Pitx2* [37–39,41].

Functional interactions between PCP proteins are important for their asymmetric distribution in the L–R organizer. In mice, the anterior localization of *Vangl2* is dependent on *Prickle1* and *Prickle2* [34]. Dachshous protocadherins have been shown to exert a permissive effect on cellular polarization. The combined loss of *Dchs1* and *Dchs2* disrupts the A–P distributions of *Vangl1* and *Vangl2* in pit cells of the node, inhibiting the left-sided expression of *Nodal* gene in the lateral plate mesoderm without affecting its expression in the node [36]. In *Xenopus*, there is evidence showing that the reciprocal interactions between *Prickle3* and *Vangl2* are required for their localization to the anterior borders of gastrocoel roof plate cells, which contributes to promoting the growth and posterior tilting of motile cilia [42]. In the zebrafish KV, JNK activity functions in Wnt/PCP signaling to establish the L–R axis. While JNK1 and JNK2 modulate ciliogenesis and cilia length to generate fluid flow in the KV and restrict left-sided expression of the *Nodal*-related gene *southpaw* in the lateral plate mesoderm, JNK3 acts downstream of JNK1 to confine the expression of *pitx2c* on the left side for specification of endodermal organs [43,44]. Overall, these observations demonstrate a critical role for Wnt/PCP signaling in the asymmetric orientation of motile cilia within the L–R organizer. Therefore, the A–P polarization of PCP proteins is translated into L–R asymmetry through biased positioning of motile cilia and their clockwise rotational motion to generate leftward fluid flow [45].

Wnt/PCP signaling also acts in concert with other regulators of the L–R asymmetry to polarize cilia and fluid flow in the L–R organizer. *Myo1D* is an unconventional myosin that plays an essential role in the control of the L–R asymmetry and the dextral rotation of visceral organs [46,47]. In zebrafish and *Xenopus*, *Myo1D* and *Vangl2* functionally interact and exert opposing effects to differentially restrict the orientation of cilia within the L–R organizer, thereby shaping a productive fluid flow and promoting the left-sided gene expression in the lateral plate mesoderm [48,49]. However, *Myo1D* can also function independently of Wnt/PCP signaling. It contributes to the formation of a spherical lumen for correct fluid flow in the zebrafish KV through fluid filling, by promoting directed vacuole trafficking in the apical membrane of KV epithelial cells [50].

4. Cilia-Driven Leftward *Nodal* Flow Initiates the L–R Asymmetry

The A–P polarity of the L–R organizer, created by the differential subcellular localization of PCP proteins and the asymmetric orientation of motile cilia, breaks the bilateral symmetry through cilia-dependent leftward fluid flow and an increase of calcium concentrations [36]. Calcium signaling then triggers differential L–R gene expression patterns and initiates the L–R asymmetry [11]. Subsequently, the left-sided expression of the *Nodal*–*Lefty*–*Pitx2* network will influence the asymmetric organ morphogenesis [23–25]. However, it seems that the vertebrate L–R organizers break the bilateral symmetry in a manner that is both cilia-dependent and independent. While cilia-driven fluid flow clearly contributes to the determination of the L–R asymmetry in *Xenopus*, zebrafish and mice, its function in the chick embryo remains largely elusive (Figure 2).

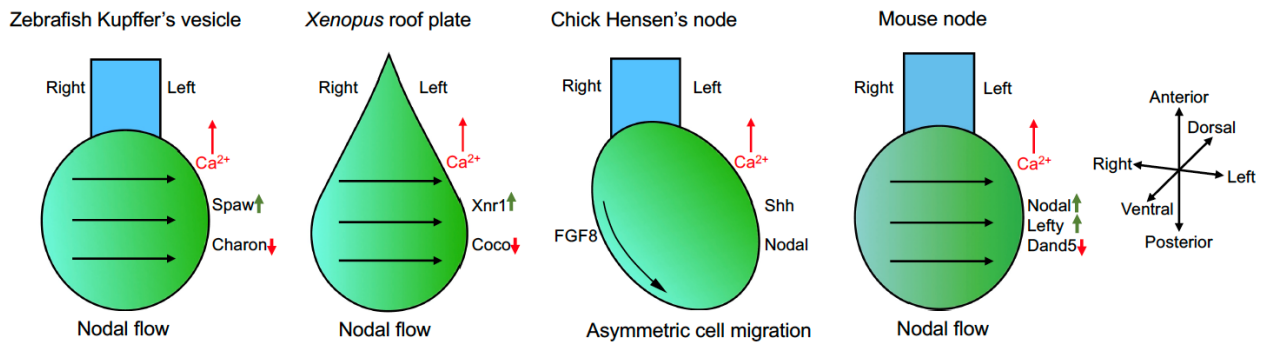


Figure 2. The L–R organizers in vertebrates. The zebrafish Kupffer’s vesicle, *Xenopus* posterior roof plate, chick Hensen’s node and mouse node are L–R organizers that function to establish the L–R asymmetry. By cilia-driven Nodal flow that triggers an increased calcium concentration on the left side (zebrafish, *Xenopus* and mouse) or by asymmetric cell migration (chick), the organizers activate differential gene expression across the L–R axis. As an outcome of calcium signaling, the reduced activity of Nodal signaling antagonists (Charon, Coco, and Dand5) leads to an increased expression of Nodal pathway genes on the left side of the lateral plate mesoderm. Upward pointing arrows indicate an increase of concentration or expression; downward arrows indicate a decreased expression.

Nodal flow leads to an increased calcium concentration on the left border of the L–R organizer, and immotile cilia function as flow sensors to initiate asymmetric calcium signaling [51]. Consequently, this results in the left-sided expression of several genes, such as *Lefty* and *Nodal* in mice, *southpaw* in zebrafish, and *Xnr1* in *Xenopus* [20]. In the chick embryo, there is no evidence indicating Nodal flow, suggesting the lack of a requirement for cilia function [52]. However, it has been shown that cilia are present at Hensen’s node between the dorsal epiblast and the ventral endoderm [53]. In addition, increased extracellular calcium levels have been detected on the left side of Hensen’s node, which is correlated with the expression of *Nodal* and *Shh* on the left side and fibroblast growth factor 8 (*Fgf8*) on the right side [54]. Nevertheless, functional assays are necessary to discriminate whether cilia trigger fluid flow and how the flow is sensed to establish asymmetric gene expression around the Hensen’s node. Although the presence, type, and function of cilia in the avian L–R organizer remain controversial, it is relatively well established that asymmetric cell migration plays an important role in breaking the bilateral symmetry. There is evidence that asymmetric bilateral counter-rotating cellular flows, termed as “polonaise” movements, occur prior to the formation of the Hensen’s node and display a right dominance [55]. It has also been shown that cells expressing *Shh* and *Fgf8* around the Hensen’s node undergo rearrangements and exhibit transient leftward movements after the full elongation and before the regression of the primitive streak, leading to asymmetric expression of these genes with respect to the midline [56,57]. Interestingly, an appropriate level of N-cadherin is important for the leftward movements to occur within this specific time window [58].

The importance of Nodal flow in breaking the bilateral symmetry has been well documented in different species [59,60]. Pioneer works show that disruption of Nodal flow in mice due to the absence of motile cilia causes randomization in the expression of flow target genes and prevents the establishment of the L–R asymmetry [21]. Interestingly, a sufficiently rapid artificial rightward flow can counteract the intrinsic leftward Nodal flow and cause situs inversus in wild-type embryos, whereas an artificial leftward flow can direct situs solitus in mutant mice with defective motile cilia [22]. Surprisingly, although 200–300 rotational cilia are present in the mouse node, there is evidence showing that as few as two motile cilia are sufficient to generate a local leftward flow and promote the formation of the L–R asymmetry [61]. This seems to suggest that there is a threshold of a weak, but nevertheless sensitive, unidirectional Nodal flow that is sufficient to trigger the left signal. Analyses in zebrafish indicate that 30 out of 200 functional motile cilia are required for situs solitus [62]. Since fewer motile cilia would only generate a weak

flow, the above observations raise the possibility that Nodal flow may be perceived as a mechanical force. Consistently, recent studies suggest that the mechanical properties of Nodal flow are responsible for breaking the bilateral symmetry. In the zebrafish KV, fluid replacement experiments indicate that the L–R organizer is sensitive to fluid dynamics instead of fluid content [63]. However, as discussed below, there are also arguments supporting the existence of a morphogen gradient generated by fluid flow across the mediolateral plane. Indeed, although the observation that two rotating cilia are able to trigger fluid flow may favor the mechanical force model, it cannot exclude the possibility that there may be still left-sided transport of chemical cues.

Intriguingly, the clockwise rotational movement of motile cilia in the mouse node not only depends on their posterior tilting coordinated by Wnt/PCP signaling but is also regulated by the absence of the radial spoke, a multi-unit protein structure present at the center of the axoneme. The knockout of *Rsph4a*, which encodes a component of the axonemal radial spoke head, transforms the planar beating of airway cilia into a clockwise rotation and promotes the clockwise rotation of node cilia [64,65]. This observation leads to the speculation that mouse node cilia have lost radial spokes during evolution and lack the central structure, although fewer 9 + 2 type cilia are still present [64,65]. There are also several lines of evidence indicating that the disruption of structural and functional components of axonemal microtubules causes defective unidirectional rotation of cilia. Disturbing the regular arrangement of doublet microtubules in mouse node cilia prevents their stable clockwise rotation [64]. The mutations of different axonemal dynein proteins lead to a loss of cilia motility and L–R patterning defects in mice and humans [66–68]. Similarly, kinesin family members of microtubule motors are required for ciliary morphogenesis. Thus, the knockout of *Kif3A* or *Kif3B* in mice leads to the absence of all cilia in the node and randomized L–R asymmetry [21,69,70]. The defective cilia phenotype can be observed at E7.5, before the earliest expression of L–R asymmetric genes [69], suggesting that motile and immotile cilia contribute to the initial determination of the L–R asymmetry. In addition, overexpression of a mutated tubulin protein in *Xenopus* perturbs the sidedness of L–R asymmetric gene expression, but whether this affects cilia formation and motility is not clear [71].

5. Calcium Signaling in L–R Axis Patterning

The left-sided activation of calcium signaling plays a conserved role in L–R asymmetry formation, but the molecular mechanisms are still under intensive investigations. In the mouse node, calcium signals can be detected on the left margin of the node coincident with Nodal flow [51,72,73]. Pharmacological inhibition of calcium signals alters early asymmetric gene expression and disrupts L–R axis formation [72]. In the zebrafish KV, left-biased intraciliary calcium oscillations are linked to the activation of downstream L–R signaling and molecular asymmetry [74]. Reducing calcium influx or the suppression of intraciliary calcium oscillations disrupts L–R patterning [74,75]. Functional analyses of calcium-sensitive channels also strongly implicate calcium signaling in L–R axis development. The calcium-permeable cation channel Polycystin-2 (PC2), encoded by the *Pkd2* gene, is a six-pass transmembrane protein and a member of the transient receptor potential (TRP) channel family. Mutations of the *PKD2* gene in humans are responsible for autosomal dominant polycystic kidney disease (ADPKD). PC2 not only functions as a cation-permeant and calcium-sensitive channel, but also acts as a regulator of other channels, contributing to intracellular signaling [76]. It is present in both motile and immotile cilia but seems to be preferentially localized to immotile cilia in crown cells [51]. PC2 is clearly involved in modulating calcium signaling to differentially regulate L–R gene expression (Figure 3). In zebrafish and mice, the loss of PC2 function disrupts asymmetric calcium signaling associated with the defective expression of L–R genes [51,77–79]. The knockdown of *Pkd2* in *Xenopus* also causes the absence of fluid flow and prevents the left-sided activation of a Nodal signaling cascade [80]. Nevertheless, it seems that PC2 exerts different effects on Nodal expression in mice and zebrafish. Mouse *Pkd2* mutants lack a left-specific calcium

expression at the node and show a complete absence of Nodal expression in the lateral plate mesoderm [51,77], while zebrafish *pkd2* mutants display a bilateral activation of *southpaw* expression in the lateral plate mesoderm [78]. Thus, PC2 in mice triggers an asymmetric calcium transient to activate the left-sided Nodal expression, while it may function to restrict the Nodal expression on the left side in zebrafish. In addition, it has also been suggested that *pkd2* deficiency in zebrafish may reduce cilia length and indirectly affect Nodal flow dynamics [81].

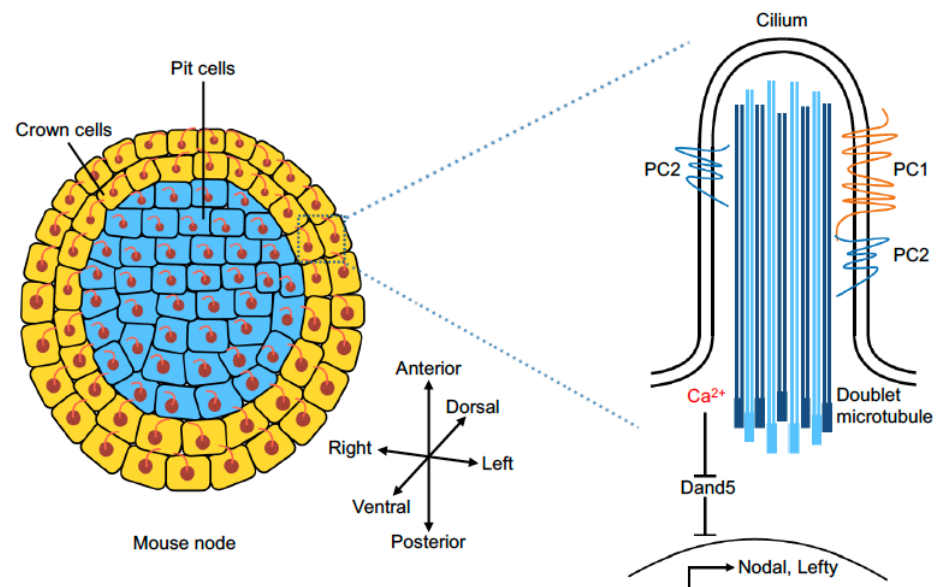


Figure 3. Organization and signaling of the mouse L–R organizer. Located at the posterior end of the notochord, the mouse node consists of pit cells (blue) at the central depression and crown cells (orange) at the periphery. The clockwise (ventral view) rotational movements of posteriorly tilted motile cilia on pit cells generates Nodal flow and causes an increased calcium concentration on the left side. Primary cilia on crown cells sense Nodal flow to activate calcium signaling, which represses the left-sided expression of *Dand5* through a post-transcriptional mechanism. Polycystin 1 (PC1) and Polycystin 2 (PC2) are enriched in immotile cilia. They may form a heteromeric ion channel complex to mediate flow-induced activation or repression of gene expression by functioning as a mechanosensor and/or chemosensor.

Although the elevated calcium signaling on the left side of vertebrate L–R organizers is indispensable for the differential expression of laterality genes across the L–R axis, the mechanism by which cilia perceive this information is not fully understood and remains a subject of debate. Using fluorescent calcium indicators, asymmetric intraciliary calcium oscillations have been observed in the zebrafish KV and the mouse node, which are tightly linked to L–R asymmetric gene expression and determination [72–74]. Despite the presence of calcium transients on both sides of the mouse node, quantitative analysis indicates that the mean frequency of calcium spikes is two-fold higher on the left side than on the right side [73]. Both in zebrafish and mice, the preferential left-sided calcium oscillations are clearly dependent on the function of PC2 [73,74]. It is well established that calcium oscillations control the efficiency and specificity of gene expression in a variety of processes [82]. Several mechanisms may be involved in differentially regulating gene expression on the left and right sides. Signaling pathways regulated by Ca²⁺/calmodulin-dependent protein kinase II (CaMKII), which is localized to cilia and required for L–R in zebrafish [83], may be activated by intraciliary calcium oscillations to mediate gene transcription. Calcium ion is also an important regulator of protein charge and conformation [84]; thus, it can function as a potent second message to regulate many signaling pathways, leading to the transcriptional, post-transcriptional, or post-translational activation of gene expression. Other targets of the intraciliary calcium signaling may include adenylyl cyclase (AC) which

influences the level of cAMP [85], as well as Inversion (Inv), which contains Calmodulin-binding IQ domains and is involved in the control of L–R asymmetry [86,87]. There is also evidence that the intracellular tail of PC1 becomes cleaved following mechanical stimuli; PC2 modulates its nuclear translocation and transcriptional activity [88,89]. Despite this progress, future studies are necessary to identify the targets of these signaling mechanisms and determine how they differentially regulate gene expression for L–R axis specification. It should be mentioned that there is still some discrepancy regarding calcium increase in primary cilia. One study has failed to detect calcium transients in the mouse node, raising the possibility that ciliary function may be regulated by calcium propagation from the cytoplasm into the cilium [90].

6. Mechanosensor and Chemosensor of Fluid Flow

How is Nodal flow sensed in the L–R organizer? At present, two hypotheses have been proposed to explain this important phenomenon: mechanosensor and chemosensor models [20]. The mechanosensor model suggests that bending of the axoneme in immotile cilia caused by fluid flow can trigger the activation of intraciliary calcium flux and subsequent asymmetric gene expression on the left side. Indeed, mechanical oscillation of cilia stimulated by optical tweezers is sufficient to induce intraciliary calcium transients in a PC2-dependent manner [91,92]. In the mouse node, it seems that PC2 is enriched at the dorsal side of immotile cilia [93]. Fluid flow causes the asymmetric deformation of immotile cilia along the D–V axis, and calcium flux can be induced by ventrally directed mechanical force [92]. In the zebrafish KV, PC2 also mediates intraciliary calcium transients, and interestingly, situs inversus in mutant fish lacking motile cilia can be rescued by applying mechanical force to immotile cilia [91]. Polycystin-1 (PC1), an eleven-pass transmembrane protein, is also a member of the TRP channel family and is responsible for ADPKD in humans [94]. It may associate with PC2 in a heteromeric complex to mediate ion permeation of the cilia, although PC2 can also function as a homomeric complex [20]. The PC1 class of the TRP channel includes PC1L1, PC1L2, and PC1L3, encoded by *Pkd111*, *Pkd112*, and *Pkd113*, respectively. The knockout of *pkd111* in zebrafish leads to the bilateral activation of Nodal expression, suggesting that PC1L1 normally functions to restrict left-sided Nodal expression [95]. However, the loss of PC1L1 and PC2 in mice produces opposite effects. Mechanistically, PC1L1 may antagonize the function of PC2 and mediate a response to Nodal flow through mechanosensation [95]. These findings demonstrate a mechanosensory function of immotile cilia, which interprets Nodal flow in a manner that requires the correct localization of PC2. Nevertheless, as aforementioned, experiments targeting calcium sensors to the cytoplasm and cilia suggest that mechanical forces do not directly evoke intraciliary calcium signaling, thus questioning whether primary cilia in general are calcium-responsive sensors [90]. Therefore, further investigations are necessary to determine the regulatory mechanisms of ciliary mechanosensation.

The chemosensor model proposes that Nodal flow generates a gradient of putative morphogens or activators of laterality genes to specify the initial L–R axis [96]. It has been shown that Shh- and retinoic acid-containing secreted extracellular vesicles, termed as “Nodal vesicular parcels”, are transported to the left side of the mouse node by fluid flow, thus establishing a L–R gradient of morphogens [97]. Intriguingly, these extracellular vesicles also contain PC1L1 protein, which is transferred to crown cells on the left side of the node where it forms a functional complex with PC2 to mediate calcium elevation on the left margin [98]. This is consistent with several lines of evidence showing that PC1L1 and PC2 establish the L–R asymmetry through physical interaction and interdependent colocalization to the cilium [99,100]. Although it is unclear how PC1L1-containing exosomes are secreted into the node cavity, the PC1L1-PC2 complex clearly plays a chemosensory role to mediate calcium elevation and signaling [20]. Thus, how cilia sense Nodal flow to activate left-sided gene expression remains a topic of heated debate. There may also be a species-specific reception and interpretation of Nodal flow. In zebrafish, it has been documented that the very limited numbers of immotile cilia present in the KV are not

sufficient to mediate mechanosensing for robust determination of the L–R asymmetry; however, motile cilia may be able to mechanically sense their own motion to generate an asymmetric response or absorb secreted signaling molecules first present on the left side [101]. Based on experimental data and computational modeling [101], it cannot be excluded that chemical signal and mechanical stimulation may function in parallel to establish the L–R asymmetry.

7. Flow-Induced Differential L–R Gene Expression

Although there are many unanswered questions in both mechanosensor and chemosensor models [20,102], Polycystin proteins are clearly essential in sensitizing crown cells and evoking calcium signaling. The link between calcium signaling and asymmetric gene expression is also enigmatic, but early molecular events triggered by flow-mediated signal(s) are beginning to be elucidated. *Dand5*, also known as *Cerl2* or *Cer2*, functions as an extracellular antagonist of Nodal protein by preventing the formation of heterodimers between Nodal and *Gdf1* [103]. It is the first asymmetrically expressed gene involved in L–R patterning [61,104], and its mRNA is selectively degraded in crown cells on the left side of the mouse node, resulting in expression on the right side [105]. Interestingly, the RNA-binding protein, *Bicc1* (Bicaudal C), which is also required for L–R patterning [106], binds to the 3′-UTR of *Dand5* mRNA to promote its degradation at the left side in two-somite stage embryos [107,108]. As a result, this leads to an increased Nodal activity and the consequent expression of Nodal, *Lefty*, and *Pitx2* on the left side of the lateral plate mesoderm [11]. Thus, *Dand5* represents an early flow target gene with an important role in establishing the gene expression network for L–R patterning [109,110]. In *Bicc1* mutant mice, the expression of *Lefty1*, *Lefty2*, and *Pitx2* becomes bilateral, inverted, or absent [106]. Similarly, the loss of *Dand5* in mice causes the bilateral and right-sided expression of *Lefty2* and *Pitx2* [105]. Although the midline expression of *Lefty1* does not seem to be affected, it becomes more pronounced in the node and predominantly localizes to the posterior side [87,105,106]. Since *Lefty1* inhibits Nodal function, this ectopic expression of *Lefty1* in the node should perturb the onset of asymmetric Nodal signaling in the lateral plate mesoderm [87]. Therefore, the post-transcriptionally controlled local degradation of *Dand5* is critical for the proper activation of the Nodal program in the lateral plate mesoderm [111]. Nevertheless, the mechanisms by which ciliary signaling activates or represses left-sided gene expression require further investigation.

There is also evidence that Wnt/ β -catenin signaling contributes to regulating the asymmetric expression of *Dand5* [112] because Wnt-*Dand5* interlinked feedback loops can enhance the leftward flow [113]. *Wnt3* exhibits L–R differences in expression and promotes the decay of *Dand5* mRNA in crown cells on the left side, while *Dand5* can also induce *Wnt3* degradation [113]. Thus, the differential activation and repression of gene expression establishes L–R embryonic polarity that will influence asymmetric organ morphogenesis.

8. Randomization of L–R Asymmetry and Laterality Defects

The molecular asymmetry established in the early embryos contributes in part to the asymmetric organ development. Therefore, the mutation or dysregulation of genes involved in the morphogenesis of the L–R organizer is closely linked to laterality disorders [26,27]. Because the heart is the first formed functional organ and undergoes asymmetric morphogenesis during development, it is not surprising that defective function of the L–R organizer frequently causes heterotaxy and congenital heart disease [114]. As aforementioned, Wnt/PCP signaling is required for the asymmetric positioning of cilia in the L–R organizer. Its dysfunction is tightly associated with congenital disorders affecting proper organogenesis [9,115]. Randomized positioning of cilia in the node due to mutations of PCP genes in mice, such as *Vangl2*, impairs Nodal flow, leads to reversal of *Lefty1/2* expression and bilateral *Pitx2* expression in the lateral plate mesoderm, and causes defective rightward looping of the heart tube [38,39]. The *Zic3* transcription factor is expressed in the mouse node but not in the heart; however, its loss of function not only affects L–R pattern-

ing but also leads to heart laterality disorders [116]. There is evidence that *Zic3* functions early in L–R organizer development by regulating the expression of PCP genes [117,118]. In humans, frameshift, missense, and nonsense mutations of the *ZIC3* gene cause X-linked situs abnormalities ranging from heterotaxy to situs ambiguus or situs inversus [119]. *Myo1D* regulates cilia orientation and Nodal flow in concert with or independently of Wnt/PCP signaling [47–49]. A rare novel missense variant of *MYO1D* gene has been linked to polysplenia syndrome presenting visceral heterotaxy and left isomerism [120]. In addition, single cell sequencing of the mouse L–R organizer has identified potential novel heterotaxy-related genes, which may be useful for studying the genetic cause of laterality disorders [121]. Thus, functional analysis of these genes not only helps decipher the mechanism underlying laterality establishment but also contributes to understanding the genetic cause of heterotaxy.

The loss of structural or signaling components in L–R organizer-related cilia also severely affects asymmetric cardiac morphogenesis. Indeed, mutagenesis screen in mice indicate that congenital heart disease (CHD) genes are related to cilia function or cilia-mediated signal transduction, such as *Shh*, Wnt/PCP components, calcium signaling, and vesicular trafficking. Importantly, many of these genes overlap with *de novo* coding mutations identified in human CHD patients [122,123]. For example, homozygous splicing and missense mutations of *PKD1L1* in humans are associated with heterotaxy or situs inversus totalis and congenital cardiac malformations [124]. It is also worth mentioning that mutations of flow target genes, such as *PITX2*, may cause CHD in the absence of laterality defects, suggesting an important and broad role of L–R patterning in the pathogenesis of CHD [122,123]. In addition, dynein dysfunction, as a cause of primary ciliary dyskinesia and other ciliopathies, is clearly associated with laterality defects in humans [125]. Although variants with a loss of kinesin gene function are responsible for many so-called ‘kinesinopathies’ presenting with congenital malformations [126], further investigations are necessary to determine whether they are linked to situs abnormalities.

9. Conclusions and Perspectives

Extensive studies have significantly contributed to understanding the intricate processes that establish the L–R asymmetry, although there are still many intriguing unanswered questions (Figure 4). Importantly, the L–R organizer is indispensable for breaking the initial bilateral symmetry. It is well established that the conserved Wnt/PCP signaling pathway contributes to setting up the biased orientation and rotational motion of motile cilia within the L–R organizer in most species. However, whether there exists an interaction between Wnt/PCP signaling and cilia in initiating the bilateral asymmetry in the chick embryo remains largely elusive and requires further functional investigations. Another key issue concerns the regulatory mechanisms by which asymmetric calcium signaling is initiated within the L–R organizer. Although the two-cilia model suggests that immotile cilia sense Nodal flow generated by motile cilia [127], the identity of the flow input remains a subject of hot debate. In the mouse node, for example, several studies suggest the existence of left-sided intraciliary calcium oscillations triggered by Nodal flow, which are closely linked to the determination of the L–R asymmetry [72–74]; however, there are also experiments indicating the absence of calcium-responsive sensors in immotile cilia [90]. Adding to this complexity, it remains to be determined whether Nodal flow is sensed as mechanical forces or chemical cues. The fact that intraciliary calcium flux can be initiated by direct application of mechanical stimulus to a cilium, and that the weak unidirectional flow triggered by two rotating cilia is sufficient to break L–R symmetry, seems to support the mechanosensory model [61,91,92]. On the other hand, it should take into account the possibility that morphogen-based chemical cues may function independently of and/or in parallel with mechanical forces to initiate left–right asymmetric gene expression [95,96]. Therefore, the regulatory mechanisms of ciliary signaling await further investigations. There exists also a gap in understanding the molecular pathways connecting elevated calcium levels and downstream gene expression events. *PC1L1* and

PC2 may be important for mediating calcium signaling in regulating the expression of flow target genes, although the mechanism remains unclear. It is known that Nodal flow leads to the leftward degradation of *Dand5* mRNA, thereby preventing the expression of Dand5 protein and its antagonizing activity on Nodal signaling on the left side [113]. The post-transcriptional regulation mediated by RNA-binding proteins may contribute to the differential expression of *Dand5* [106,108]. For a better mechanistic understanding of how calcium signaling is initiated and how it differentially activates or represses gene expression on the left or right side, it is important to develop new tools for monitoring intraciliary calcium changes that may be triggered by flow-associated mechanical and/or chemical cues. Further studies are also required to identify intraciliary calcium signaling networks responsible for L–R asymmetric gene expression at transcriptional, post-transcriptional, and post-translational levels.

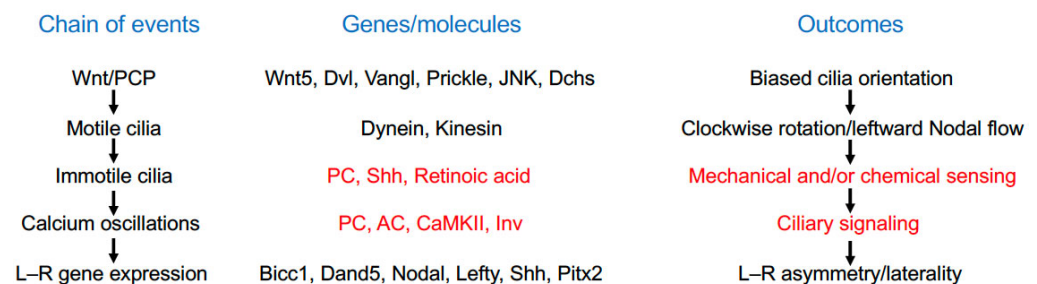


Figure 4. Brief summary of the temporal process leading to the determination of the L–R asymmetry. Further studies for elucidating the underlying mechanisms of ciliary functions are highlighted in red. The list of genes involved in the chain of events are not exhaustive. PC, Polycystin; AC, adenylyl cyclase; CaMKII, Ca²⁺/calmodulin-dependent protein kinase II; Inv, Inversion.

The mutations of genes involved in L–R axis formation are closely associated with laterality defects in animal models and in humans. However, besides microtubule motors dyneins, mutations of only a few genes functioning in the L–R organizer have been associated with human laterality defects. The identification of novel genes expressed in this transient embryonic structure could facilitate genetic screening of congenital malformations in humans. A better understanding of the genetic cascade that controls L–R axis formation not only will contribute to deciphering the mechanism underlying asymmetric organ morphogenesis, but should also help to develop strategies for the diagnosis of congenital disease, particularly heart malformations.

Funding: This research was funded by the French Muscular Dystrophy Association (AFM-Téléthon grant number 23545), the annual supports from the Centre National de la Recherche Scientifique (CNRS), and the Sorbonne University, and the APC was funded by CNRS and Sorbonne Université.

Institutional Review Board Statement: Not applicable.

Informed Consent Statement: Not applicable.

Data Availability Statement: No new data were created in this work.

Conflicts of Interest: The author declares no conflicts of interest.

References

- Carron, C.; Shi, D.L. Specification of anteroposterior axis by combinatorial signaling during *Xenopus* development. *Wiley Interdiscip. Rev. Dev. Biol.* **2016**, *5*, 150–168. [[CrossRef](#)] [[PubMed](#)]
- Shi, D.L. Canonical and non-canonical Wnt signaling generates molecular and cellular asymmetries to establish embryonic axes. *J. Dev. Biol.* **2024**, *12*, 20. [[CrossRef](#)] [[PubMed](#)]
- Matsui, T.; Bessho, Y. Left-right asymmetry in zebrafish. *Cell. Mol. Life Sci.* **2012**, *69*, 3069–3077. [[CrossRef](#)] [[PubMed](#)]
- Nakamura, T.; Hamada, H. Left-right patterning: Conserved and divergent mechanisms. *Development* **2012**, *139*, 3257–3262. [[CrossRef](#)]

5. Vandenberg, L.N.; Levin, M. A unified model for left-right asymmetry? Comparison and synthesis of molecular models of embryonic laterality. *Dev. Biol.* **2013**, *379*, 1–15. [[CrossRef](#)]
6. Coutelis, J.B.; González-Morales, N.; Géminard, C.; Noselli, S. Diversity and convergence in the mechanisms establishing L/R asymmetry in metazoa. *EMBO Rep.* **2014**, *15*, 926–937. [[CrossRef](#)]
7. Hamada, H. Molecular and cellular basis of left-right asymmetry in vertebrates. *Proc. Jpn. Acad. Ser. B Phys. Biol. Sci.* **2020**, *96*, 273–296. [[CrossRef](#)]
8. Kuroda, R. Left-right asymmetry in invertebrates: From molecules to organisms. *Annu. Rev. Cell Dev. Biol.* **2024**, *40*, 97–117. [[CrossRef](#)]
9. Shi, D.L. Planar cell polarity regulators in asymmetric organogenesis during development and disease. *J. Genet. Genom.* **2023**, *50*, 63–76. [[CrossRef](#)]
10. Yoshida, S.; Hamada, H. Roles of cilia, fluid flow, and Ca²⁺ signaling in breaking of left-right symmetry. *Trends Genet.* **2014**, *30*, 10–17. [[CrossRef](#)]
11. Grimes, D.T.; Burdine, R.D. Left-right patterning: Breaking symmetry to asymmetric morphogenesis. *Trends Genet.* **2017**, *33*, 616–628. [[CrossRef](#)] [[PubMed](#)]
12. Hamada, H.; Tam, P. Diversity of left-right symmetry breaking strategy in animals. *F1000Research* **2020**, *9*, F1000. [[CrossRef](#)] [[PubMed](#)]
13. Little, R.B.; Norris, D.P. Right, left and cilia: How asymmetry is established. *Semin. Cell Dev. Biol.* **2021**, *110*, 11–18. [[CrossRef](#)] [[PubMed](#)]
14. Katoh, T.A. Function of nodal cilia in left-right determination: Mechanical regulation in initiation of symmetry breaking. *Biophys. Physicobiol.* **2024**, *21*, e210018. [[CrossRef](#)]
15. Wang, Y.; Nathans, J. Tissue/planar cell polarity in vertebrates: New insights and new questions. *Development* **2007**, *134*, 647–658. [[CrossRef](#)]
16. Gray, R.S.; Roszko, I.; Solnica-Krezel, L. Planar cell polarity: Coordinating morphogenetic cell behaviors with embryonic polarity. *Dev. Cell* **2011**, *21*, 120–133. [[CrossRef](#)]
17. Axelrod, J.D. Planar cell polarity signaling in the development of left-right asymmetry. *Curr. Opin. Cell Biol.* **2020**, *62*, 61–69. [[CrossRef](#)]
18. Minegishi, K.; Sai, X.; Hamada, H. Role of Wnt signaling and planar cell polarity in left-right asymmetry. *Curr. Top. Dev. Biol.* **2023**, *153*, 181–193. [[CrossRef](#)]
19. Langenbacher, A.; Chen, J.N. Calcium signaling: A common thread in vertebrate left-right axis development. *Dev. Dyn.* **2008**, *237*, 3491–3496. [[CrossRef](#)]
20. Tajhya, R.; Delling, M. New insights into ion channel-dependent signalling during left-right patterning. *J. Physiol.* **2020**, *598*, 1741–1752. [[CrossRef](#)]
21. Nonaka, S.; Tanaka, Y.; Okada, Y.; Takeda, S.; Harada, A.; Kanai, Y.; Kido, M.; Hirokawa, N. Randomization of left-right asymmetry due to loss of nodal cilia generating leftward flow of extraembryonic fluid in mice lacking KIF3B motor protein. *Cell* **1998**, *95*, 829–837. [[CrossRef](#)]
22. Nonaka, S.; Shiratori, H.; Saijoh, Y.; Hamada, H. Determination of left-right patterning of the mouse embryo by artificial nodal flow. *Nature* **2002**, *418*, 96–99. [[CrossRef](#)]
23. Mercola, M.; Levin, M. Left-right asymmetry determination in vertebrates. *Annu. Rev. Cell Dev. Biol.* **2001**, *17*, 779–805. [[CrossRef](#)]
24. Raya, A.; Izpisua Belmonte, J.C. Left-right asymmetry in the vertebrate embryo: From early information to higher-level integration. *Nat. Rev. Genet.* **2006**, *7*, 283–293. [[CrossRef](#)]
25. Grimes, D.T. Making and breaking symmetry in development, growth and disease. *Development* **2019**, *146*, dev170985. [[CrossRef](#)]
26. Capdevila, I.; Izpisua Belmonte, J.C. Knowing left from right: The molecular basis of laterality defects. *Mol. Med. Today* **2000**, *6*, 112–118. [[CrossRef](#)]
27. Forrest, K.; Barricella, A.C.; Pohar, S.A.; Hinman, A.M.; Amack, J.D. Understanding laterality disorders and the left-right organizer: Insights from zebrafish. *Front. Cell Dev. Biol.* **2022**, *10*, 1035513. [[CrossRef](#)]
28. Gao, B. Wnt regulation of planar cell polarity (PCP). *Curr. Top. Dev. Biol.* **2012**, *101*, 263–295. [[CrossRef](#)]
29. Wallingford, J.B. Planar cell polarity and the developmental control of cell behavior in vertebrate embryos. *Annu. Rev. Cell Dev. Biol.* **2012**, *28*, 627–653. [[CrossRef](#)]
30. Yang, Y.; Mlodzik, M. Wnt-Frizzled/planar cell polarity signaling: Cellular orientation by facing the wind (Wnt). *Annu. Rev. Cell Dev. Biol.* **2015**, *31*, 623–646. [[CrossRef](#)]
31. Henderson, D.J.; Long, D.A.; Dean, C.H. Planar cell polarity in organ formation. *Curr. Opin. Cell Biol.* **2018**, *55*, 96–103. [[CrossRef](#)] [[PubMed](#)]
32. Blair, S.; McNeill, H. Big roles for Fat cadherins. *Curr. Opin. Cell Biol.* **2018**, *51*, 73–80. [[CrossRef](#)] [[PubMed](#)]
33. Milgrom-Hoffman, M.; Humbert, P.O. Regulation of cellular and PCP signalling by the Scribble polarity module. *Semin. Cell Dev. Biol.* **2018**, *81*, 33–45. [[CrossRef](#)] [[PubMed](#)]
34. Minegishi, K.; Hashimoto, M.; Ajima, R.; Takaoka, K.; Shinohara, K.; Ikawa, Y.; Nishimura, H.; McMahon, A.P.; Willert, K.; Okada, Y.; et al. A Wnt5 activity asymmetry and intercellular signaling via PCP proteins polarize node cells for left-right symmetry breaking. *Dev. Cell* **2017**, *40*, 439–452.e4. [[CrossRef](#)]

35. Hashimoto, M.; Shinohara, K.; Wang, J.; Ikeuchi, S.; Yoshiba, S.; Meno, C.; Nonaka, S.; Takada, S.; Hatta, K.; Wynshaw-Boris, A.; et al. Planar polarization of node cells determines the rotational axis of node cilia. *Nat. Cell Biol.* **2010**, *12*, 170–176. [[CrossRef](#)]
36. Sai, X.; Ikawa, Y.; Nishimura, H.; Mizuno, K.; Kajikawa, E.; Katoh, T.A.; Kimura, T.; Shiratori, H.; Takaoka, K.; Hamada, H.; et al. Planar cell polarity-dependent asymmetric organization of microtubules for polarized positioning of the basal body in node cells. *Development* **2022**, *149*, dev200315. [[CrossRef](#)]
37. Antic, D.; Stubbs, J.L.; Suyama, K.; Kintner, C.; Scott, M.P.; Axelrod, J.D. Planar cell polarity enables posterior localization of nodal cilia and left-right axis determination during mouse and *Xenopus* embryogenesis. *PLoS ONE* **2010**, *5*, e8999. [[CrossRef](#)]
38. Song, H.; Hu, J.; Chen, W.; Elliott, G.; Andre, P.; Gao, B.; Yang, Y. Planar cell polarity breaks bilateral symmetry by controlling ciliary positioning. *Nature* **2010**, *466*, 378–382. [[CrossRef](#)]
39. Mahaffey, J.P.; Grego-Bessa, J.; Liem, K.F., Jr.; Anderson, K.V. Cofilin and Vangl2 cooperate in the initiation of planar cell polarity in the mouse embryo. *Development* **2013**, *140*, 1262–1271. [[CrossRef](#)]
40. Borovina, A.; Superina, S.; Voskas, D.; Ciruna, B. Vangl2 directs the posterior tilting and asymmetric localization of motile primary cilia. *Nat. Cell Biol.* **2010**, *12*, 407–412. [[CrossRef](#)]
41. Zhang, Y.; Levin, M. Left-right asymmetry in the chick embryo requires core planar cell polarity protein Vangl2. *Genesis* **2009**, *47*, 719–728. [[CrossRef](#)] [[PubMed](#)]
42. Chu, C.W.; Ossipova, O.; Ioannou, A.; Sokol, S.Y. Prickle3 synergizes with Wtip to regulate basal body organization and cilia growth. *Sci. Rep.* **2016**, *6*, 24104. [[CrossRef](#)] [[PubMed](#)]
43. Derrick, C.J.; Santos-Ledo, A.; Eley, L.; Henderson, D.J.; Chaudhry, B. Sequential action of jnk genes establishes the embryonic left-right axis. *Development* **2022**, *149*, dev200136. [[CrossRef](#)] [[PubMed](#)]
44. Gao, Q.; Zhang, J.; Wang, X.; Liu, Y.; He, R.; Liu, X.; Wang, F.; Feng, J.; Yang, D.; Wang, Z.; et al. The signalling receptor MCAM coordinates apical-basal polarity and planar cell polarity during morphogenesis. *Nat. Commun.* **2017**, *8*, 15279. [[CrossRef](#)]
45. Hashimoto, M.; Hamada, H. Translation of anterior-posterior polarity into left-right polarity in the mouse embryo. *Curr. Opin. Genet. Dev.* **2010**, *20*, 433–437. [[CrossRef](#)]
46. Hozumi, S.; Maeda, R.; Taniguchi, K.; Kanai, M.; Shirakabe, S.; Sasamura, T.; Spéder, P.; Noselli, S.; Aigaki, T.; Murakami, R.; et al. An unconventional myosin in *Drosophila* reverses the default handedness in visceral organs. *Nature* **2006**, *440*, 798–802. [[CrossRef](#)]
47. Spéder, P.; Adám, G.; Noselli, S. Type ID unconventional myosin controls left-right asymmetry in *Drosophila*. *Nature* **2006**, *440*, 803–807. [[CrossRef](#)]
48. Juan, T.; Géminard, C.; Coutelis, J.B.; Cerezo, D.; Polès, S.; Noselli, S.; Fürthauer, M. Myosin1D is an evolutionarily conserved regulator of animal left-right asymmetry. *Nat. Commun.* **2018**, *9*, 1942. [[CrossRef](#)]
49. Tingler, M.; Kurz, S.; Maerker, M.; Ott, T.; Fuhl, F.; Schweickert, A.; LeBlanc-Straceski, J.M.; Noselli, S.; Blum, M. A conserved role of the unconventional Myosin 1d in laterality determination. *Curr. Biol.* **2018**, *28*, 810–816.e3. [[CrossRef](#)]
50. Saydmohammed, M.; Yagi, H.; Calderon, M.; Clark, M.J.; Feinstein, T.; Sun, M.; Stolz, D.B.; Watkins, S.C.; Amack, J.D.; Lo, C.W.; et al. Vertebrate myosin 1d regulates left-right organizer morphogenesis and laterality. *Nat. Commun.* **2018**, *9*, 3381. [[CrossRef](#)]
51. McGrath, J.; Somlo, S.; Makova, S.; Tian, X.; Brueckner, M. Two populations of node monocilia initiate left-right asymmetry in the mouse. *Cell* **2003**, *114*, 61–73. [[CrossRef](#)] [[PubMed](#)]
52. Blum, M.; Weber, T.; Beyer, T.; Vick, P. Evolution of leftward flow. *Semin. Cell Dev. Biol.* **2009**, *20*, 464–471. [[CrossRef](#)] [[PubMed](#)]
53. Essner, J.J.; Vogan, K.J.; Wagner, M.K.; Tabin, C.J.; Yost, H.J.; Brueckner, M. Conserved function for embryonic nodal cilia. *Nature* **2002**, *418*, 37–38. [[CrossRef](#)] [[PubMed](#)]
54. Raya, A.; Kawakami, Y.; Rodríguez-Esteban, C.; Ibañes, M.; Rasskin-Gutman, D.; Rodríguez-León, J.; Büscher, D.; Feijó, J.A.; Izpisua Belmonte, J.C. Notch activity acts as a sensor for extracellular calcium during vertebrate left-right determination. *Nature* **2004**, *427*, 121–128. [[CrossRef](#)]
55. Asai, R.; Sinha, S.; Prakash, V.N.; Mikawa, T. Bilateral cellular flows display asymmetry prior to left-right organizer formation in amniote gastrulation. *bioRxiv* **2024**. [[CrossRef](#)]
56. Cui, C.; Little, C.D.; Rongish, B.J. Rotation of organizer tissue contributes to left-right asymmetry. *Anat. Rec. Adv. Integr. Anat. Evol. Biol.* **2009**, *292*, 557–561. [[CrossRef](#)]
57. Gros, J.; Feistel, K.; Viebahn, C.; Blum, M.; Tabin, C.J. Cell movements at Hensen’s node establish left/right asymmetric gene expression in the chick. *Science* **2009**, *324*, 941–944. [[CrossRef](#)]
58. Mendes, R.V.; Martins, G.G.; Cristovão, A.M.; Saúde, L. N-cadherin locks left-right asymmetry by ending the leftward movement of Hensen’s node cells. *Dev. Cell* **2014**, *30*, 353–360. [[CrossRef](#)]
59. Hirokawa, N.; Tanaka, Y.; Okada, Y.; Takeda, S. Nodal flow and the generation of left-right asymmetry. *Cell* **2006**, *125*, 33–45. [[CrossRef](#)]
60. Blum, M.; Feistel, K.; Thumberger, T.; Schweickert, A. The evolution and conservation of left-right patterning mechanisms. *Development* **2014**, *141*, 1603–1613. [[CrossRef](#)]
61. Shinohara, K.; Kawasumi, A.; Takamatsu, A.; Yoshiba, S.; Botilde, Y.; Motoyama, N.; Reith, W.; Durand, B.; Shiratori, H.; Hamada, H. Two rotating cilia in the node cavity are sufficient to break left-right symmetry in the mouse embryo. *Nat. Commun.* **2012**, *3*, 622. [[CrossRef](#)] [[PubMed](#)]

62. Sampaio, P.; Ferreira, R.R.; Guerrero, A.; Pintado, P.; Tavares, B.; Amaro, J.; Smith, A.A.; Montenegro-Johnson, T.; Smith, D.J.; Lopes, S.S. Left-right organizer flow dynamics: How much cilia activity reliably yields laterality? *Dev. Cell* **2014**, *29*, 716–728. [[CrossRef](#)] [[PubMed](#)]
63. Sampaio, P.; Pestana, S.; Bota, C.; Guerrero, A.; Telley, I.A.; Smith, D.; Lopes, S.S. Fluid extraction from the left-right organizer uncovers mechanical properties needed for symmetry breaking. *Elife* **2023**, *12*, e83861. [[CrossRef](#)] [[PubMed](#)]
64. Shinohara, K.; Chen, D.; Nishida, T.; Misaki, K.; Yonemura, S.; Hamada, H. Absence of radial spokes in mouse node cilia is required for rotational movement but confers ultrastructural instability as a trade-off. *Dev. Cell* **2015**, *35*, 236–246. [[CrossRef](#)]
65. Shinohara, K.; Hamada, H. Cilia in left-right symmetry breaking. *Cold Spring Harb. Perspect. Biol.* **2017**, *9*, a028282. [[CrossRef](#)]
66. Supp, D.M.; Witte, D.P.; Potter, S.S.; Brueckner, M. Mutation of an axonemal dynein affects left-right asymmetry in inversus viscerum mice. *Nature* **1997**, *389*, 963–966. [[CrossRef](#)]
67. Supp, D.M.; Brueckner, M.; Kuehn, M.R.; Witte, D.P.; Lowe, L.A.; McGrath, J.; Corrales, J.; Potter, S.S. Targeted deletion of the ATP binding domain of left-right dynein confirms its role in specifying development of left-right asymmetries. *Development* **1999**, *126*, 5495–5504. [[CrossRef](#)]
68. Olbrich, H.; Häffner, K.; Kispert, A.; Völkel, A.; Volz, A.; Sasmaz, G.; Reinhardt, R.; Hennig, S.; Lehrach, H.; Konietzko, N.; et al. Mutations in DNAH5 cause primary ciliary dyskinesia and randomization of left-right asymmetry. *Nat. Genet.* **2002**, *30*, 143–144. [[CrossRef](#)]
69. Marszalek, J.R.; Ruiz-Lozano, P.; Roberts, E.; Chien, K.R.; Goldstein, L.S. Situs inversus and embryonic ciliary morphogenesis defects in mouse mutants lacking the KIF3A subunit of kinesin-II. *Proc. Natl. Acad. Sci. USA* **1999**, *96*, 5043–5048. [[CrossRef](#)]
70. Takeda, S.; Yonekawa, Y.; Tanaka, Y.; Okada, Y.; Nonaka, S.; Hirokawa, N. Left-right asymmetry and kinesin superfamily protein KIF3A: New insights in determination of laterality and mesoderm induction by kif3A^{-/-} mice analysis. *J. Cell Biol.* **1999**, *145*, 825–836. [[CrossRef](#)]
71. Lobikin, M.; Wang, G.; Xu, J.; Hsieh, Y.W.; Chuang, C.F.; Lemire, J.M.; Levin, M. Early, nonciliary role for microtubule proteins in left-right patterning is conserved across kingdoms. *Proc. Natl. Acad. Sci. USA* **2012**, *109*, 12586–12591. [[CrossRef](#)] [[PubMed](#)]
72. Takao, D.; Nemoto, T.; Abe, T.; Kiyonari, H.; Kajjura-Kobayashi, H.; Shiratori, H.; Nonaka, S. Asymmetric distribution of dynamic calcium signals in the node of mouse embryo during left-right axis formation. *Dev. Biol.* **2013**, *376*, 23–30. [[CrossRef](#)] [[PubMed](#)]
73. Mizuno, K.; Shiozawa, K.; Katoh, T.A.; Minegishi, K.; Ide, T.; Ikawa, Y.; Nishimura, H.; Takaoka, K.; Itabashi, T.; Iwane, A.H.; et al. Role of Ca²⁺ transients at the node of the mouse embryo in breaking of left-right symmetry. *Sci. Adv.* **2020**, *6*, eaba1195. [[CrossRef](#)]
74. Yuan, S.; Zhao, L.; Brueckner, M.; Sun, Z. Intraciliary calcium oscillations initiate vertebrate left-right asymmetry. *Curr. Biol.* **2015**, *25*, 556–567. [[CrossRef](#)]
75. Sarmah, B.; Latimer, A.J.; Appel, B.; Wente, S.R. Inositol polyphosphates regulate zebrafish left-right asymmetry. *Dev. Cell* **2005**, *9*, 133–145. [[CrossRef](#)]
76. Brill, A.L.; Ehrlich, B.E. Polycystin 2: A calcium channel, channel partner, and regulator of calcium homeostasis in ADPKD. *Cell. Signal.* **2020**, *66*, 109490. [[CrossRef](#)]
77. Pennekamp, P.; Karcher, C.; Fischer, A.; Schweickert, A.; Skryabin, B.; Horst, J.; Blum, M.; Dworniczak, B. The ion channel polycystin-2 is required for left-right axis determination in mice. *Curr. Biol.* **2002**, *12*, 938–943. [[CrossRef](#)]
78. Schottenfeld, J.; Sullivan-Brown, J.; Burdine, R.D. Zebrafish curly up encodes a Pkd2 ortholog that restricts left-side-specific expression of southpaw. *Development* **2007**, *134*, 1605–1615. [[CrossRef](#)]
79. Yoshida, S.; Shiratori, H.; Kuo, I.Y.; Kawasumi, A.; Shinohara, K.; Nonaka, S.; Asai, Y.; Sasaki, G.; Belo, J.A.; Sasaki, H.; et al. Cilia at the node of mouse embryos sense fluid flow for left-right determination via Pkd2. *Science* **2012**, *338*, 226–231. [[CrossRef](#)]
80. Vick, P.; Kreis, J.; Schneider, I.; Tingler, M.; Getwan, M.; Thumberger, T.; Beyer, T.; Schweickert, A.; Blum, M. An early function of Polycystin-2 for left-right organizer induction in *Xenopus*. *iScience* **2018**, *2*, 76–85. [[CrossRef](#)]
81. Jacinto, R.; Sampaio, P.; Roxo-Rosa, M.; Pestana, S.; Lopes, S.S. Pkd2 affects cilia length and impacts LR flow dynamics and Dand5. *Front. Cell Dev. Biol.* **2021**, *9*, 624531. [[CrossRef](#)] [[PubMed](#)]
82. Dolmetsch, R.E.; Xu, K.; Lewis, R.S. Calcium oscillations increase the efficiency and specificity of gene expression. *Nature* **1998**, *392*, 933–936. [[CrossRef](#)] [[PubMed](#)]
83. Francescato, L.; Rothschild, S.C.; Myers, A.L.; Tombes, R.M. The activation of membrane targeted CaMK-II in the zebrafish Kupffer's vesicle is required for left-right asymmetry. *Development* **2010**, *137*, 2753–2762. [[CrossRef](#)] [[PubMed](#)]
84. Clapham, D.E. Calcium signaling. *Cell* **2007**, *131*, 1047–1058. [[CrossRef](#)]
85. Sun, Z. Regulation and Function of Calcium in the Cilium. *Curr. Opin. Physiol.* **2020**, *17*, 278–283. [[CrossRef](#)]
86. Mochizuki, T.; Saijoh, Y.; Tsuchiya, K.; Shirayoshi, Y.; Takai, S.; Taya, C.; Yonekawa, H.; Yamada, K.; Nihei, H.; Nakatsuji, N.; et al. Cloning of *inv*, a gene that controls left/right asymmetry and kidney development. *Nature* **1998**, *395*, 177–181. [[CrossRef](#)]
87. Oki, S.; Kitajima, K.; Marques, S.; Belo, J.A.; Yokoyama, T.; Hamada, H.; Meno, C. Reversal of left-right asymmetry induced by aberrant Nodal signaling in the node of mouse embryos. *Development* **2009**, *136*, 3917–3925. [[CrossRef](#)]
88. Arnould, T.; Kim, E.; Tsiokas, L.; Jochimsen, F.; Grüning, W.; Chang, J.D.; Walz, G. The polycystic kidney disease 1 gene product mediates protein kinase C alpha-dependent and c-Jun N-terminal kinase-dependent activation of the transcription factor AP-1. *J. Biol. Chem.* **1998**, *273*, 6013–6018. [[CrossRef](#)]
89. Chauvet, V.; Tian, X.; Husson, H.; Grimm, D.H.; Wang, T.; Hiesberger, T.; Igarashi, P.; Bennett, A.M.; Ibraghimov-Beskrovnaya, O.; Somlo, S.; et al. Mechanical stimuli induce cleavage and nuclear translocation of the polycystin-1 C terminus. *J. Clin. Investig.* **2004**, *114*, 1433–1443. [[CrossRef](#)]

90. Delling, M.; Indzhykulia, A.A.; Liu, X.; Li, Y.; Xie, T.; Corey, D.P.; Clapham, D.E. Primary cilia are not calcium-responsive mechanosensors. *Nature* **2016**, *531*, 656–660. [[CrossRef](#)]
91. Djenoune, L.; Mahamdeh, M.; Truong, T.V.; Nguyen, C.T.; Fraser, S.E.; Brueckner, M.; Howard, J.; Yuan, S. Cilia function as calcium-mediated mechanosensors that instruct left-right asymmetry. *Science* **2023**, *379*, 71–78. [[CrossRef](#)] [[PubMed](#)]
92. Katoh, T.A.; Omori, T.; Mizuno, K.; Sai, X.; Minegishi, K.; Ikawa, Y.; Nishimura, H.; Itabashi, T.; Kajikawa, E.; Hiver, S.; et al. Immotile cilia mechanically sense the direction of fluid flow for left-right determination. *Science* **2023**, *379*, 66–71. [[CrossRef](#)] [[PubMed](#)]
93. Katoh, T.A.; Lange, T.; Nakajima, Y.; Yashiro, K.; Okada, Y.; Hamada, H. BMP4 regulates asymmetric Pkd2 distribution in mouse nodal immotile cilia and ciliary mechanosensing required for left-right determination. *Dev. Dyn.* **2024**. [[CrossRef](#)] [[PubMed](#)]
94. Fedeles, S.V.; Gallagher, A.R.; Somlo, S. Polycystin-1: A master regulator of intersecting cystic pathways. *Trends Mol. Med.* **2014**, *20*, 251–260. [[CrossRef](#)]
95. Grimes, D.T.; Keynton, J.L.; Buenavista, M.T.; Jin, X.; Patel, S.H.; Kyosuke, S.; Vibert, J.; Williams, D.J.; Hamada, H.; Hussain, R.; et al. Genetic analysis reveals a hierarchy of interactions between polycystin-encoding genes and genes controlling cilia function during left-right determination. *PLoS Genet.* **2016**, *12*, e1006070. [[CrossRef](#)]
96. Okada, Y.; Nonaka, S.; Tanaka, Y.; Saijoh, Y.; Hamada, H.; Hirokawa, N. Abnormal nodal flow precedes situs inversus in iv and inv mice. *Mol. Cell* **1999**, *4*, 459–468. [[CrossRef](#)]
97. Tanaka, Y.; Okada, Y.; Hirokawa, N. FGF-induced vesicular release of Sonic hedgehog and retinoic acid in leftward nodal flow is critical for left-right determination. *Nature* **2005**, *435*, 172–177. [[CrossRef](#)]
98. Tanaka, Y.; Morozumi, A.; Hirokawa, N. Nodal flow transfers polycystin to determine mouse left-right asymmetry. *Dev. Cell* **2023**, *58*, 1447–1461.e6. [[CrossRef](#)]
99. Field, S.; Riley, K.L.; Grimes, D.T.; Hilton, H.; Simon, M.; Powles-Glover, N.; Siggers, P.; Bogani, D.; Greenfield, A.; Norris, D.P. Pkd11l1 establishes left-right asymmetry and physically interacts with Pkd2. *Development* **2011**, *138*, 1131–1142. [[CrossRef](#)]
100. Kamura, K.; Kobayashi, D.; Uehara, Y.; Koshida, S.; Iijima, N.; Kudo, A.; Yokoyama, T.; Takeda, H. Pkd11l1 complexes with Pkd2 on motile cilia and functions to establish the left-right axis. *Development* **2011**, *138*, 1121–1129. [[CrossRef](#)]
101. Ferreira, R.R.; Vilfan, A.; Jülicher, F.; Supatto, W.; Vermot, J. Physical limits of flow sensing in the left-right organizer. *eLife* **2017**, *6*, e25078. [[CrossRef](#)] [[PubMed](#)]
102. Wachten, D.; Mill, P. The cilia mechanosensation debate gets (bio)physical. *Nat. Rev. Nephrol.* **2023**, *19*, 279–280. [[CrossRef](#)] [[PubMed](#)]
103. Tanaka, C.; Sakuma, R.; Nakamura, T.; Hamada, H.; Saijoh, Y. Long-range action of Nodal requires interaction with GDF1. *Genes Dev.* **2007**, *21*, 3272–3282. [[CrossRef](#)] [[PubMed](#)]
104. Schweickert, A.; Vick, P.; Getwan, M.; Weber, T.; Schneider, I.; Eberhardt, M.; Beyer, T.; Pachur, A.; Blum, M. The nodal inhibitor Coco is a critical target of leftward flow in *Xenopus*. *Curr. Biol.* **2010**, *20*, 738–743. [[CrossRef](#)]
105. Marques, S.; Borges, A.C.; Silva, A.C.; Freitas, S.; Cordenonsi, M.; Belo, J.A. The activity of the Nodal antagonist Cerl-2 in the mouse node is required for correct L/R body axis. *Genes Dev.* **2004**, *18*, 2342–2347. [[CrossRef](#)]
106. Maisonneuve, C.; Guilleret, I.; Vick, P.; Weber, T.; Andre, P.; Beyer, T.; Blum, M.; Constam, D.B. Bicaudal C, a novel regulator of Dvl signaling abutting RNA-processing bodies, controls cilia orientation and leftward flow. *Development* **2009**, *136*, 3019–3030. [[CrossRef](#)]
107. Maerker, M.; Getwan, M.; Dowdle, M.E.; McSheene, J.C.; Gonzalez, V.; Pelliccia, J.L.; Hamilton, D.S.; Yartseva, V.; Vejnar, C.; Tingler, M.; et al. Bic1 and Dicer regulate left-right patterning through post-transcriptional control of the Nodal inhibitor Dand5. *Nat. Commun.* **2021**, *12*, 5482. [[CrossRef](#)]
108. Minegishi, K.; Rothé, B.; Komatsu, K.R.; Ono, H.; Ikawa, Y.; Nishimura, H.; Katoh, T.A.; Kajikawa, E.; Sai, X.; Miyashita, E.; et al. Fluid flow-induced left-right asymmetric decay of Dand5 mRNA in the mouse embryo requires a Bic1-Ccr4 RNA degradation complex. *Nat. Commun.* **2021**, *12*, 4071. [[CrossRef](#)]
109. Hashimoto, H.; Rebagliati, M.; Ahmad, N.; Muraoka, O.; Kurokawa, T.; Hibi, M.; Suzuki, T. The Cerberus/Dan-family protein Charon is a negative regulator of Nodal signaling during left-right patterning in zebrafish. *Development* **2004**, *131*, 1741–1753. [[CrossRef](#)]
110. Montague, T.G.; Gagnon, J.A.; Schier, A.F. Conserved regulation of Nodal-mediated left-right patterning in zebrafish and mouse. *Development* **2018**, *145*, dev171090. [[CrossRef](#)]
111. Belo, J.A.; Marques, S.; Inácio, J.M. The role of Cerl2 in the establishment of left-right asymmetries during axis formation and heart development. *J. Cardiovasc. Dev. Dis.* **2017**, *4*, 23. [[CrossRef](#)] [[PubMed](#)]
112. Kitajima, K.; Oki, S.; Ohkawa, Y.; Sumi, T.; Meno, C. Wnt signaling regulates left-right axis formation in the node of mouse embryos. *Dev. Biol.* **2013**, *380*, 222–232. [[CrossRef](#)] [[PubMed](#)]
113. Nakamura, T.; Saito, D.; Kawasumi, A.; Shinohara, K.; Asai, Y.; Takaoka, K.; Dong, F.; Takamatsu, A.; Belo, J.A.; Mochizuki, A.; et al. Fluid flow and interlinked feedback loops establish left-right asymmetric decay of Cerl2 mRNA. *Nat. Commun.* **2012**, *3*, 1322. [[CrossRef](#)] [[PubMed](#)]
114. Wells, J.R.; Padua, M.B.; Ware, S.M. The genetic landscape of cardiovascular left-right patterning defects. *Curr. Opin. Genet. Dev.* **2022**, *75*, 101937. [[CrossRef](#)]
115. Shi, D.L. Wnt/planar cell polarity signaling controls morphogenetic movements of gastrulation and neural tube closure. *Cell. Mol. Life Sci.* **2022**, *79*, 586. [[CrossRef](#)]

116. Sutherland, M.J.; Wang, S.; Quinn, M.E.; Haaning, A.; Ware, S.M. Zic3 is required in the migrating primitive streak for node morphogenesis and left-right patterning. *Hum. Mol. Genet.* **2013**, *22*, 1913–1923. [[CrossRef](#)]
117. Winata, C.L.; Kondrychyn, I.; Kumar, V.; Srinivasan, K.G.; Orlov, Y.; Ravishankar, A.; Prabhakar, S.; Stanton, L.W.; Korzh, V.; Mathavan, S. Genome wide analysis reveals Zic3 interaction with distal regulatory elements of stage specific developmental genes in zebrafish. *PLoS Genet.* **2013**, *9*, e1003852. [[CrossRef](#)]
118. Bellchambers, H.M.; Ware, S.M. Loss of Zic3 impairs planar cell polarity leading to abnormal left-right signaling, heart defects and neural tube defects. *Hum. Mol. Genet.* **2021**, *30*, 2402–2415. [[CrossRef](#)]
119. Bellchambers, H.M.; Ware, S.M. ZIC3 in heterotaxy. *Adv. Exp. Med. Biol.* **2018**, *1046*, 301–327. [[CrossRef](#)]
120. Alsafwani, R.S.; Nasser, K.K.; Shinawi, T.; Banaganapalli, B.; ElSokary, H.A.; Zaher, Z.F.; Shaik, N.A.; Abdelmohsen, G.; Al-Aama, J.Y.; Shapiro, A.J.; et al. Novel MYO1D missense variant identified through whole exome sequencing and computational biology analysis expands the spectrum of causal genes of laterality defects. *Front. Med.* **2021**, *8*, 724826. [[CrossRef](#)]
121. Bellchambers, H.M.; Phatak, A.R.; Nenni, M.J.; Padua, M.B.; Gao, H.; Liu, Y.; Ware, S.M. Single cell RNA analysis of the left-right organizer transcriptome reveals potential novel heterotaxy genes. *Sci. Rep.* **2023**, *13*, 10688. [[CrossRef](#)] [[PubMed](#)]
122. Li, Y.; Klena, N.T.; Gabriel, G.C.; Liu, X.; Kim, A.J.; Lemke, K.; Chen, Y.; Chatterjee, B.; Devine, W.; Damerla, R.R.; et al. Global genetic analysis in mice unveils central role for cilia in congenital heart disease. *Nature* **2015**, *521*, 520–524. [[CrossRef](#)] [[PubMed](#)]
123. Gabriel, G.C.; Young, C.B.; Lo, C.W. Role of cilia in the pathogenesis of congenital heart disease. *Semin. Cell Dev. Biol.* **2021**, *110*, 2–10. [[CrossRef](#)]
124. Vetrini, F.; D'Alessandro, L.C.; Akdemir, Z.C.; Braxton, A.; Azamian, M.S.; Eldomery, M.K.; Miller, K.; Kois, C.; Sack, V.; Shur, N.; et al. Bi-allelic mutations in PKD1L1 are associated with laterality defects in humans. *Am. J. Hum. Genet.* **2016**, *99*, 886–893. [[CrossRef](#)]
125. Despotes, K.A.; Zariwala, M.A.; Davis, S.D.; Ferkol, T.W. Primary ciliary dyskinesia: A clinical review. *Cells* **2024**, *13*, 974. [[CrossRef](#)]
126. Kalantari, S.; Filges, I. 'Kinesinopathies': Emerging role of the kinesin family member genes in birth defects. *J. Med. Genet.* **2020**, *57*, 797–807. [[CrossRef](#)]
127. Tabin, C.J.; Vogan, K.J. A two-cilia model for vertebrate left-right axis specification. *Genes Dev.* **2003**, *17*, 1–6. [[CrossRef](#)]

Disclaimer/Publisher's Note: The statements, opinions and data contained in all publications are solely those of the individual author(s) and contributor(s) and not of MDPI and/or the editor(s). MDPI and/or the editor(s) disclaim responsibility for any injury to people or property resulting from any ideas, methods, instructions or products referred to in the content.